Demonstration of Remote Clock Monitoring by VLBI, With Three Baseline Closure

C. M. Cheetham, W. J. Hurd, and J. W. Layland[1]
Communications Systems Research Section

G. A. Madrid and T. P. Yunck
Navigation Systems Section

The capability of very long baseline interferometry (VLBI) to monitor the stability of remotely-located hydrogen maser frequency standards has been demonstrated by a series of experiments conducted from September 1978, through January 1979, between Deep Space Stations in Australia, Spain, and California. The measured stabilities of the clock systems, over approximately 10-day intervals, were 1 to 3 parts in 10^{13}, with the instabilities due to the oscillators, the clock distribution systems, the receiving system delays, and the VLBI measurement error.

Experiments were conducted independently using two different systems (BLOCK 0 and WBDAS). Later comparison shows agreement in the order of 1 part in 10^{13}. Closure was demonstrated on three separate occasions to 33, 10, and 13 ns with an error uncertainty of ±42 ns. The results clearly demonstrate the resolution and consistency of VLBI measurements.

I. Introduction

In order to improve the quality of radiometric observables at outer planet distances, the monitoring of time offsets and frequency standards at DSN tracking stations has become a necessity. Very long baseline interferometry (VLBI) presents the most promising technique available to monitor clock epoch and rate offsets to the level required for advanced deep space missions. The feasibility of such an application has been independently demonstrated at JPL by Goldstein in 1967 (Ref. 1), Hurd in 1972 (Refs. 2-5), and Thomas, et al., in 1974 (Ref. 6). Using current technology the technique has the potential of determining frequency standard rates to 1 part in 10^{13} with a few minutes of observing time and to 1 part in 10^{14} over periods of approximately 1 week, by differencing clock offset estimates.

This article reports the results of a series of clock synchronization experiments that were conducted from September 1978 through January 1979, between DSSs in

[1] Now with TDA Planning Office.

Australia, Spain, and California. During this entire time, the cesium clock at DSS 63 in Spain and the hydrogen maser clock at DSS 43 in Australia drifted only a few microseconds with respect to the DSS 14 hydrogen maser clock at Goldstone, California. The measured stabilities of the clock systems were 1 to 3 parts in 10^{13}, with the instabilities due to the oscillators, the clock distribution systems, the receiving system delays, and the VLBI measurement error.

On three separate occasions, measurements were made between the Spain and Australia stations – the first VLBI measurements ever made on this extremely long baseline. Unfortunately, these experiments could not be conducted concurrently with measurements on the other baselines. However, the data were compared to clock offsets on the other two baselines, interpolated or extrapolated to the time of the Spain-Australia measurements. These experiments demonstrated closure to 33, 10, and 13 ns, with an error budget of ±42 ns. This is a powerful demonstration of the consistency of VLBI measurements.

Two different VLBI systems were utilized in parallel in the reported experiments, thus providing both redundancy and a comparison of the two systems. The main distinction between the two systems lies in the manner in which the digitized received energy signals are recorded and correlated. One application records the digitized signal across the entire received bandwidth at distinct intervals of time, the other records selected channels across the bandwidth in a continuous stream of data from which the phase delay across the bandwidth is then reconstructed. The first mode has accordingly been termed the "Wide Band Data Acquisition System" (WBDAS) (Refs. 4 and 5) while the second is termed the "Bandwidth Synthesis" System (BWS) (Refs. 6–9). The WBDAS approach was developed strictly for near-real-time clock and frequency monitoring, requiring a minimum amount of data. The BWS technique was developed to fully utilize the maximum recording rate of available recorders, with the intent of providing a technology base for use in the DSN that could be used not only for clock synchronization, but also for determining the station geodynamic parameters required for improved spacecraft navigation (i.e., earth rotation rate and crustal motion), and for improving the positional estimates of the extragalactic radio sources to be used to conduct VLBI experiments.

The specific BWS system used in these experiments is the Block 0 system, utilizing 4-Mbit/s digital recording on video tape recorders. This is an interim system leading to DSN implementation of a near-real-time Block I BWS System, and a wider bandwidth Block II System. At the time of these experiments, the DSN stations did not have phase calibrators (Ref. 10) and cable stabilizers that will be part of the Block I and Block II Systems, and that are required to do clock synchronization with the BWS technique. Thus clock synchronization with the Block 0 system could not use BWS, but used only the bit alignment of individual channels and therefore was similar in concept to the operation of the WBDAS.

II. Experiment Configuration

The two VLBI systems used in the experiments are briefly described in this section, and the configuration of the two VLBI data acquisition systems (Fig. 1) within the DSSs is discussed. It is argued that instabilities in the station 1-pps signal supplied to the VLBI systems, and in generation of VLBI epoch references from the 1-pps inputs, are probably the dominant cause of discrepancies between results for the two systems.

A. Signal Path

The signal from the radio source passes through the antenna system and a traveling wave maser (TWM) amplifier, and is then translated from the RF center frequency to 55 MHz, using reference frequencies generated from the station frequency standard. Both VLBI systems receive 55 MHz IF signals, but there is one more stage of amplification and filtering for the WBDAS than for the Block 0 System. This restricts the passband to 55 ± 18 MHz, whereas the signal to the Block 0 System is bandwidth limited by the TWM or by a 55 ± 36 MHz filter. The difference in group delays between the two systems is consistent from experiment to experiment at a level considered to be insignificant. The total signal delay does vary significantly from experiment to experiment, however. Variations in tuning of the TWM amplifiers can cause group delay variations of ±10 ns at each station, and the path length difference between the two TWMs at each station is as much as 52 ns, including waveguide lengths. Unfortunately, no accurate record of the TWM configurations was kept for all experiments, although each station was instructed to use the same TWM for each experiment whenever possible.

B. Block 0 System

Block 0 is a bandwidth synthesis VLBI system using 4-Mbit/s digital recording on video tape recorders and sampling sequentially up to eight BWS channels, each 1.8 MHz wide. The system is designed to measure fringe rates directly and group delay by either single channel bit stream alignment or bandwidth synthesis. Because the numerical differentiation inherent in bandwidth synthesis requires precise phase coherence between the channels, the group delays produced by that method are not meaningful without the incorporation of phase calibrators to remove instrumental effects. Since operational phase calibrators were not available for these experiments, the

group delays reported here were measured from the alignment offset of a single 1.8-MHz channel and are referenced to the Block 0 sampling clocks. As described below, the timing system implementation may have resulted in experiment-to-experiment delay changes which would not have occurred if the system had been in its BWS mode with phase calibrators. The system noise effects ranged from 3–20 ns, compared to the 0.1 ns which would be achieved with BWS.

For these experiments the system was configured to sample three S-band channels, spending 0.5 second in each. Although frequently X-band data were recorded as well, they were not included in these results.

C. Wideband System

The wideband VLBI data acquisition system utilizes a high instantaneous sampling rate in order to observe the entire signal bandwidth, as limited only by the receiving system. The receiver output is digitally modulated to baseband by sampling at 50 MHz in each of the two phase-quadrature analog-to-digital (A/D) converters. The time delay observable is the differential group delay to the A/D converter sampling clocks. The A/D converter outputs are low-pass filtered, by summing N consecutive samples in a digital integrate-and-dump filter. These experiments typically used $N = 3$, thus reducing the effective bandwidth to 16-2/3 MHz. The filter outputs are quantized to 1 bit, and stored in a 4096-bit buffer. When the buffer is full, sampling is inhibited and the buffer is emptied onto magnetic tape. Fourteen bursts of data are taken each second, for an average data rate of 57 kbits/s. The WBDAS achieves a lower signal-to-noise ratio than the Block 0 system because of the lower data rate, but achieves a time-delay error due to system noise of 1–5 ns, because of the wider bandwidth.

D. Station Timing

The VLBI systems are referenced to the station frequency standards through the coherent reference generator (CRG) and the time format assembly (TFA). Power to the frequency standards, the CRG, and the TFA is nominally uninterruptible, so phase and timing is in principle continuous except when catastrophic failures occur. The function of the CRG is to generate various frequency references coherently from the station standard. For the purposes of this experiment, the CRG probably does not degrade the station standard. The station 1 pps is generated from 1 MHz in redundant divider chains. Because the divider chains are constructed of obsolete and slow circuits, the 1-pps signal is reclocked by 5 MHz in the TFA. This reclocking results in possible 200-ns glitches, which have been observed at DSS 14 during the course of these experiments. Both VLBI systems initially synchronize their internal 1-pps references to the TFA 1-pps signal, and then allow the internal clocks to free run until synchronization is lost. This loss of synchronization normally occurs only when there is an interruption in power to the TFA or to a VLBI system. Such interruptions did not occur within one day's experiment, but did occur between experiments.

E. WBDAS Timing

The WBDAS 1-pps reference is generated from a 50-MHz signal from the CRG, by dividing this signal to 1 pps using emitter coupled logic (ECL). The internal 1 pps is initially synchronized to the TFA 1 pps, and thereafter the WBDAS monitors the phase difference between the TFA 1 pps and the internal 1 pps, in increments of 10 ns. The 10-ns resolution is achieved by observing the TFA signal both directly, and delayed by 10 ns. Normally the phase relationship does not change by more than 10 ns either within an experiment or between experiments. This 10-ns variation is expected, due to drifts in the WBDAS ECL circuits or in the TFA TTL circuits. Occasionally, jumps of 200 ns were observed at DSS 14; these jumps did not accumulate, but typically changed back and forth within an experiment on some days. We attribute this effect to the TFA. These jumps occurred only at DSS 14, and were always in the same direction. Therefore it is likely that the WBDAS clock was always consistently synchronized to the 50-MHz reference, within one 20-ns count interval, even when it was necessary to resynchronize due to power outages between experiments.

F. Block 0 Timing

The Block 0 VLBI System has a sampling rate of 4 Mbit/s, a frequency which is not available in the DSSs. The 4 Mbit/s is derived from 5 MHz in a phase locked loop synthesizer system. This system generates 1 MHz from the 5-MHz reference and from a 4-MHz voltage controlled oscillator (VCO), using digital dividers. The 1-MHz signals are then phase locked. A problem with this system is that the phase relationship between the 5 MHz and the 4 MHz can change up to 200 ns in increments of 50 ns upon resynchronization. Thus, power outages to the Block 0 System, and consequent resynchronization, may result in timing offsets in increments of 50 ns, in addition to the possible 200-ns TFA offset. This synchronization error is a likely source of discrepancies between the results from the two VLBI systems.

III. Results

A. Experiments

From 3 September 1978 to 21 January 1979, a total of 34 VLBI clock sync passes were scheduled. The pass durations ranged from approximately 2 hours to 25 hours. Each pass consisted of a number of runs, i.e., time spent taking data on a

particular source, separated by antenna move time. Eight of the longer passes were scheduled by the Block 0 experimenters and consisted of 2.5-minute runs. The other passes were scheduled by the WBDAS experimenters and consisted of 9-minute runs. Because the time required for setup was uncertain, runs were scheduled from the start of the pass. Thus data was not always taken on the initial runs or the final runs. Some passes were not successful at all due to equipment failures in one or both VLBI systems, or in the DSS configuration. The results in this section are the estimates of the clock offset for the successful passes.

B. Processing and Results

1. Processing. The WBDAS results were produced in two stages. The first stage correlated the data from each separate run and produced an estimate of the clock offset and its rate of change, as well as estimates of the standard deviation for each parameter. The second stage combined the estimates for each successful run in a pass and produced an estimate for the clock offset and its rate for the pass.

Table 1 contains the results of the second stage. The column labeled Date contains the nominal date of the experiment, Epoch contains the time of the clock estimate, Clock contains the clock offset, Sigma clock contains the formal uncertainty of the clock offset, Residual contains the rms residual of the runs with respect to the clock estimate for the pass, Clock rate contains the rate of change of the clock offset, Sigma clock rate contains the formal uncertainty of the clock rate, No. of observations contains the number of runs or observations in the pass that were used to produce the pass estimates.

2. Closure Results. Three of the passes were performed on the 43/63 baseline, using only the WBDAS System. This provides a consistency check on the clock offsets, since the offsets between pairs of stations should sum to zero. Because the reference time for each pass is different and the clocks are all drifting, it is necessary to make some estimates to reference these clock offsets to the same epoch. Figure 2 shows the 14/43 and 14/63 clock offsets used to make these estimates. The clock offsets are modelled by straight-line, least-square fits to the data, based on the assumption that the clocks at the three stations have constant but different frequencies. On or about 16 November, the clock at DSS 43 apparently had a sudden frequency change and so two straight-line fits are made to the 14/43 clock offset. Table 2 contains the data used to calculate the 14/43 and 14/63 fits. The rms residuals to these fits are on the order of 70 ns. The closure is to about 10 to 30 ns. It should be noted that the 14/63 data has to be extrapolated to 14 October. The earliest 14/63 experiment used here was on 23 October since the preceding experiment of 1 October deviated considerably from the straight-line fit. The hydrogen maser at DSS 63 failed in September and presumably had not settled at its final frequency on 1 October. The fact that the closure is as good as it is suggests that it had settled before 14 October.

C. Block 0 Processing and Results

In the Block 0 System, the digital video tapes are shipped from the stations to JPL, then cross-correlated in quadrature on the hardware processor at Caltech. Postcorrelation analysis is performed on the IBM 3032 at Caltech and begins with a step called "phase-tracking" in which each source observation (typically 3-9 minutes) is divided into segments 20 to 60 seconds long. Each segment is fit by least squares to a complex sinusoid giving solutions for amplitude, phase, and fringe rate. Simultaneous interpolation of fringe amplitude in the lag domain with a sin x/x function yields the single channel group delay, while cross-channel differencing of phase solutions yields the synthesized delay for each segment. A priori values for the first segment solution are taken from an initial Fourier analysis, while those for the other segments are taken from the solutions for the segment preceding.

Segment solutions are then analyzed collectively to yield a solution for the entire observation. Amplitude and alignment delay are obtained by a weighted average of segment solutions, while fringe phase and rate result from a linear fit to segment phases. A linear fit to synthesized delays gives the final synthesized delay and a direct measurement of delay rate.

In the final processing step, solutions for all observations are supplied to a global fitting program which produces, for the entire experiment, single solutions for clock offset, fringe rate, and clock rate. In addition, when the number of observations is sufficient (typically >7), the program redetermines the baseline, thus providing some compensation for errors in the a priori UT1 and PM values. Although the program can also solve for selected source positions, we did not use that feature, electing instead to discard obviously bad data.

The Block 0 data reported here are from this final processing step. The clock rate reported is that derived from fringe rate rather than from delay rate, because this is more accurate. The rate accuracy is currently limited over the short term by systematic and random effects of ionosphere, instrumentation, and modeling errors.

Table 3 contains the Block 0 results and provides the accumulated "Allan Variance" stability estimates derived from the clock offsets. Note that the accumulation has been restarted at points of major breaks or jumps in the clocks.

D. Comparison of Results

Figure 3 shows the DSS 43 minus DSS 14 clock offsets versus epoch for both the WBDAS and Block 0 Systems. The offset is nearly linear from 17 September (Epoch 22.5) to 16 November (Epoch 27.7). The hydrogen maser failed at DSS 43 between the 3 September and 11 September passes and was put back on line just before the 11 September pass. Thus the early clock offsets are not colinear with those following. As mentioned above, the WBDAS data shows a rate change on about 16 November. This rate change is not as precisely located in the Block 0 data since there was no Block 0 result from 16 November. The frequency of the DSS 43 maser was intentionally shifted in late December and thus the offsets from 20 December (Epoch 30.7) to 12 January (Epoch 32.7) have a different rate than those previous.

Figure 4 shows the DSS 63 minus DSS 14 clock offsets versus epoch for the two systems. The DSS 63 hydrogen maser was not on line until January of 1979, thus only the last two points represent a comparison of two masers. However, the data is quite linear from 23 October (Epoch 25.7) to 24 December (Epoch 30.9) while DSS 63 was on the cesium standard.

The scale of Figs. 3 and 4 permits only a coarse comparison of the two systems. However, Fig. 5 shows the 14/43 data with a linear clock estimate removed, $\hat{c} = -26.71 + 1.35 \times$ Epoch. In addition, a constant of 0.4 microseconds has been added to the Block 0 data, which represents an estimate of the difference of the signal and clock path lengths in the two systems. The rate change in the 14/43 offset mentioned above is quite obvious in Fig. 5, however it should be noted that the slope is not really negative past 16 November since the axis of Fig. 5 has a slope of 1.35×10^{-12}. There are 10 passes on the 14/43 baseline for which both systems reported results; the rms difference (after removal of the 0.4-μs offset) is 64 ns.

Figure 6 shows the 14/63 data with a linear clock estimate removed, $\hat{c} = -11.4 + 0.29 \times$ Epoch. In addition, a bias of 56 ns has been added to the Block 0 data. The rate of 0.29×10^{-12} reflects the rate observed from 23 October (Epoch 25.7) to 24 December (Epoch 31.0). Before 23 October, the points are outside the range of Fig. 6, due to station clock adjustments. A large clock jump occurred between 24 December and 16 January, so 1.1 μs was subtracted from the passes on 16 January and 21 January to keep them on Fig. 6. There were 7 passes between 23 October and 24 December for which both systems reported results. The average difference between the two systems was 56 ns and after removal of this constant, the rms difference was 105 ns. Two days, 5 November and 3 December, disturb these calculations and may be the result of clock jumps.

IV. Analysis of Results and Error Sources

The principal objectives of VLBI clock sync experiments are to determine the offset and combined stability of the station frequency standards. In the present case, with near-simultaneous results from two different VLBI systems, we can also form some conclusions about the performance of the VLBI technique itself.

On the 14/63 baseline, over the period during which the cesium standard was on line at 63, the Block 0 results show a frequency offset of 3×10^{-13} and a stability (square root Allan variance) of 2×10^{-13} with a sample standard deviation on the latter figure of 0.9×10^{-13}. The WBDAS results show comparable values of 2.7×10^{-13} for the offset and 1.2×10^{-13} for the stability. On the 14/43 baseline both sets of results show a change in frequency offset sometime in the period from mid-November to early December. A lack of Block 0 results for mid-November prevents a more accurate determination of the time of the change. Block 0 data yield an offset of 1.7×10^{-12} before the change and 8.2×10^{-13} after, with a stability over the whole interval of 3×10^{-13}. The sample standard deviation is 1×10^{-13}. From the WBDAS data, the estimated offsets are 1.7×10^{-12} before the change and 1.2×10^{-12} after, with an overall stability of 1.9×10^{-13}. The average interval between samples is approximately 10 days; however, because the intervals vary, the Allan variances must be considered nonstandard.

Because neither S/X ionosphere calibration nor instrumental phase calibration were employed in these experiments, errors in the measured clock offsets are dominated by transmission media and instrumental effects. The stability values should therefore be regarded only as loose upper bounds on the instability of the clocks themselves.

Figures 5 and 6 show the differences between the WBDAS and Block 0 measured clock offsets, after the removal of a constant bias, on the days for which both systems obtained measurements. With the exception of a few greater discrepancies, the agreement is at about the 50-ns level. In all likelihood, the larger discrepancies are due not to large random errors but rather to real temporary changes in the instrumental delays of one system with respect to the other. For example, it has been observed that reinitializing the Block 0 clock, which is routinely done, can change its epoch with respect to the station clock by several hundred nanoseconds. The phase calibration systems now being installed will remove the effects of those jumps.

The VLBI systems described here have measured the combined instability over ~10-day intervals of frequency standards separated by intercontinental distances to low parts

in 10^{13} with an uncertainty of 1 part in 10^{13}. It is known that well-maintained hydrogen masers will show a stability over such intervals of a part in 10^{14} or better. With VLBI systems now under development using dual-frequency ionosphere calibration, accurate measurement and modeling of the wet and dry components of the troposphere, instrumental phase calibration, and simultaneous solution for UTI and polar motion corrections, stability measurements of a few parts in 10^{14} should be attainable.

Although a thorough analysis of the error sources affecting the interferometer used for these experiments has not yet been completed, a preliminary set of mean value error estimates have been compiled based on prior experience with the instrument. These values are presented in Table 4 mainly to indicate the estimated relative magnitude of the errors at S-band. For the sake of consistency, the geometric effects have been scaled to a hypothetical 10,000 km. baseline and approximate worst case partials are provided as well as the corresponding one sigma error values. In the cases of "System Noise", "Instrumentation", "Ionosphere", and "Bandpass Shape", only those values footnoted by an "a" or a "c" are applicable to the current instruments. The other values presented in these categories represent an estimate of the level to which these error sources will be reduced once phase calibration and dual-frequency charged particle error cancellation have been introduced.

The system noise contribution ranges from 1 ns for strong sources with either system, to 20 ns with the Block 0 System for sources too weak to be determined with the WBDAS. The range of 10-40 ns for instrumentation effects depends on the station configuration integrity. The bandpass shape factor is smaller, about 1 ns, for the WBDAS than the 10 ns for the Block 0, due to system bandwidth utilized (Ref. 11). Since there are normally some strong radio sources in an experiment, the dominant error sources are instrumentation stability and the ionosphere, whose contributions cannot be accurately estimated. Overall, the error of the current measurements is believed to be in the range of 24-51 ns.

For the closure experiment, the expected error is $\sqrt{3}$ times the individual experiment error, or 42-88 ns, neglecting frequency stability induced errors. Thus the closures of 33, 10, and 13 ns were better than anticipated.

Acknowledgments

The authors express their appreciation to B. Bronwein, E. Cohen, R. Henderson, R. Shaffer, D. Spitzmesser, and the Deep Space Station personnel for their assistance in scheduling, configuring, and operating the stations, and processing the data.

References

1. Goldstein, R., "Clock Calibration via Quasar," in the *Space Programs Summary 34-48*. Vol. II, pp. 79-82, Jet Propulsion Laboratory, Pasadena, Calif., November 30, 1967.

2. Hurd, W. J., "A Demonstration of DSN Clock Synchronization by VLBI," in *The Deep Space Network Progress Report*, Technical Report 32-1526, Vol. XII, pp. 149-160, Jet Propulsion Laboratory, Pasadena, Calif., December 15, 1972.

3. Hurd, W. J., "An Analysis and Demonstration of Clock Synchronization by VLBI," *IEEE Transactions on Instrumentation and Measurement* Vol. IM-23, No. 1, pp. 80-89, March 1974.

4. Hurd, W. J., "Preliminary Demonstration of Precision DSN Clock Synchronization by Radio Interferometry," in the *Deep Space Network Progress Report* 42-37, Jet Propulsion Laboratory, Pasadena, Calif., February 15, 1977, pp. 57-68.

5. Hurd, W. J., et al., "Submicrosecond Comparison of Intercontinental Clock Synchronization by VLBI and the NTS Satellite," *Proceedings of the Tenth Annual Precise Time and Time Interval Applications and Planning Meeting*, NASA TM 80250, Goddard Space Flight Center, Greenbelt, MD., Nov 28-30, 1978, pp. 629-642. Also in the *Deep Space Network Progress Report*, Technical Report 32-1526, Vol. 49, pp. 64-69, Jet Propulsion Laboratory, Pasadena, Calif., February 15, 1979.

6. Thomas, J. B., et al., "Radio Interferometry Measurements of a 16 km Baseline with 4 cm Precision," in *The Deep Space Network Progress Report*, Technical Report 32-1526, Vol. XIX, pp. 36-54, Jet Propulsion Laboratory, Pasadena, Calif., February 15, 1974.

7. Thomas, J. B., "An Analysis of Long Baseline Radio Interferometry," in *The Deep Space Network Progress Report*, Technical Report 32-1526, Vol. VIII, p. 37, Jet Propulsion Laboratory, Pasadena, Calif., February 1972.

8. Thomas, J. B., "An Analysis of Long Baseline Ratio Interferometry, Part II," in *The Deep Space Network Progress Report*. Technical Report 32-1526, Vol. VIII, p. 29, Jet Propulsion Laboratory, Pasadena, Calif., May 1972.

9. Thomas, J. B., "An Analysis of Long Baseline Radio Interferometry, Part III," in *The Deep Space Network Progress Report*, Technical Report 32-1526, Vol. XVI, p. 47, Jet Propulsion Laboratory, Pasadena, Calif., August 15, 1973.

10. Thomas, J. B., "The Tone Generator and Phase Calibration in VLBI Measurements," in *The Deep Space Network Progress Report*, 42-44, Jet Propulsion Laboratory, Pasadena, Calif., February 1978, pp. 63-74.

11. Layland, J. W. and W. J. Hurd, "VLBI Instrumental Effects, Part I," in *The Deep Space Network Progress Report*, 42-42, Jet Propulsion Laboratory, Pasadena, Calif., December 1977, pp. 54-80.

Table 1. WBDAS results

Date	Epoch, secs past 1 Jan 1978 × 10^6	Clock, ns	Sigma clock, ns	Residual, ns	Clock rate, × 10^{-12}	Sigma clock rate, × 10^{-12}	No. of observations
				14/43			
11 Sep	21.9816	3.551	0.4	5.3	0.78	0.08	4
17 Sep	22.518	3.744	23.9	62.8	3.0	0.7	7
23 Sep	23.0292	4.379	18.0	–	5.0	2.0	1
30 Sep	23.6304	5.292	0.4	5.4	1.41	0.06	6
14 Oct	24.8436	7.320	0.6	2.1	3.4	0.15	2
23 Oct	25.6176	8.591	0.7	7.9	1.8	0.1	3
27 Oct	26.0064	9.316	0.2	10.9	2.28	0.007	23
4 Nov	26.6724	10.659	0.4	11.5	0.98	0.04	9
16 Nov	27.6912	12.337	0.5	5.4	1.6	0.07	4
29 Nov	28.8072	13.688	0.6	11.2	2.1	0.2	3
12 Dec	29.9808	15.125	1.1	4.3	−2.8	0.9	2
31 Dec	31.5864	16.407	0.2	8.2	0.18	0.005	14
12 Jan	32.6628	17.423	0.5	14.2	0	0.15	6
				14/63			
9 Sep	21.8484	−8.768	0.8	6.8	−1.8	0.2	5
1 Oct	23.7348	−2.443	0.15	14.8	0.7	0.4	4
23 Oct	25.6536	−3.845	0.8	7.6	−1.4	0.2	5
30 Oct	26.2008	−3.705	0.7	18.9	4.09	0.08	9
5 Nov	26.7984	−3.451	0.3	32.4	0.66	0.01	10
20 Nov	28.0044	−3.303	0.5	5.9	1.0	0.1	6
27 Nov	28.6092	−3.126	0.5	6.4	0.3	0.1	5
3 Dec	29.1996	−2.955	1.4	4.3	−0.7	0.3	5
24 Dec	30.9492	−2.368	0.3	6.0	−0.28	0.04	10
16 Jan	32.9472	−0.664	0.4	4.2	−0.5	0.07	6
21 Jan	33.3756	−0.564	0.8	4.5	−0.2	0.1	4
				43/63			
14 Oct	24.858	−11.400	1.0	18.2	−3.4	0.3	5
3 Nov	26.604	−14.033	1.0	1.4	−4.0	0.2	3
28 Nov	28.7532	−16.643	2.0	6.3	−4.0	0.6	2

Table 2. WBDAS closure results

Date	Epoch	Clock	Residual to Fit	
			14/43	
30 Sep	23.6304	5.292	0.070	$\hat{T}_{43-14}$ = −36.1159
14 Oct	24.8436	7.320	−0.025	+ 1.74937 × Epoch
23 Oct	25.6176	8.591	−0.108	rms residual = 0.076
27 Oct	26.0064	9.316	−0.063	
4 Nov	26.6724	10.659	0.115	
16 Nov	27.6912	12.337	0.011	
16 Nov	27.6912	12.337	0.003	$\hat{T}'_{43-14}$ = −21.386
29 Nov	28.8072	13.688	−0.005	+ 1.2177 × Epoch
12 Dec	29.9808	15.125	0.003	rms residual = 0.004
			14/63	
23 Oct	25.6536	−3.845	0.007	$\hat{T}_{64-14}$ = −10.669
30 Oct	26.2008	−3.705	0.001	+ 0.26574 × Epoch
5 Nov	26.7984	−3.451	0.097	rms residual = 0.062
20 Nov	28.0044	−3.303	−0.076	
27 Nov	28.6092	−3.126	−0.060	
3 Dec	29.1996	−2.955	−0.046	
24 Dec	30.9492	−2.368	0.077	
			43/63	
			$\hat{T}_{43-14}$	$\hat{T}_{63-14}$ RESID = T_{63-43} + T_{43-14} − T_{63-14}
14 Oct	24.858	−11.400	7.370	−4.063 0.033
3 Nov	26.604	−14.033	10.424	−3.599 −0.010
28 Nov	28.7532	−16.643	13.628	−3.028 0.013

Table 3. Block 0 results

Date	Epoch	Clock, μs	Sigma clock, ns	Rate, $\times 10^{-12}$	No. of observations	Square root Allan variance, $\times 10^{-13}$
			14/43			
3 Sep	21.322339	4.368	5.2	−2.38	32	–
17 Sep	22.518534	3.377	9.7	2.22	7	–
30 Sep	23.629294	4.844	1.7	1.93	5	–
14 Oct	24.844771	6.910	1.0	3.82	3	2.68
23 Oct	25.618483	8.156	4.7	3.26	4	1.95
27 Oct	25.975236	8.744	2.4	2.31	117	1.60
4 Nov	26.670332	10.317	5.0	5.96	24	2.58
29 Nov	28.806020	13.397	1.6	2.91	4	3.47
13 Dec	29.981315	14.776	6.7	1.08	3	3.26
20 Dec	30.671408	15.361	2.0	2.23	3	3.14
31 Dec	31.543594	15.955	1.7	1.68	33	2.97
13 Jan	32.662017	16.984	14.6	2.32	6	2.86
			14/63			
4 Sep	21.385637	−7.668	3.8	0.68	56	–
16 Sep	22.410587	−10.059	7.3	−5.15	59	–
23 Oct	25.655368	−3.965	8.0	−0.62	5	–
30 Oct	26.180608	−3.828	6.2	−1.82	57	–
5 Nov	26.754849	−3.672	3.9	0.24	127	0.08
20 Nov	28.005401	−3.329	9.3	0.13	7	0.06
27 Nov	28.611230	−3.184	18.9	0.09	5	0.15
3 Dec	29.202867	−2.800	7.5	1.05	3	1.45
16 Dec	30.249901	−2.604	8.0	0.16	17	1.96
24 Dec	30.942036	−2.385	5.3	0.16	15	1.82
16 Jan	32.947914	−0.582	2.1	−2.08	4	
21 Jan	33.374313	−0.469	15.5	−0.84	5	

Table 4. Estimated magnitudes of error sources at S-band for a 10,000-km baseline

Error Source	Delay			Delay rate, $x\omega$		
	Partial	1σ	Final value	Partial	1σ	Final value
Source position	130 ns/"	0.015"	2 ns	22 mHz/"	0.015"	0.33 mHz
Baseline	3.33 ns/m	1.0 m	3.33 ns	0.56 mHz/m	1.0 m	0.56 mHz
UT1	2.0 μs/sec	0.003 sec	6 ns	0.32 Hz/sec	0.003 sec	1.0 mHz
PM (X)	3.33 ns/m	0.7 m	2.3 ns	0.56 mHz/m	0.7 m	0.4 mHz
PM (Y)	3.33 ns/m	0.7 m	2.3 ns	0.45 mHz/m	0.7 m	0.4 mHz
System noise			1–20 ns[a]			2.3 mHz[a]
	n/a[b]	n/a	3.5 ns	n/a	n/a	0.4 mHz
Instrumentation			20–40 ns[a]			1.0 mHz[a]
	n/a	n/a	3 ns	n/a	n/a	0.1 mHz
Ionosphere			10–20 ns[c]			4.0 mHz[b]
	n/a	n/a	~ 0 ns	n/a	n/a	~ 0 mHz
Troposphere	n/a	n/a	1 ns	n/a	n/a	0.2 mHz
Bandpass shape			1–10 ns[a]			
	n/a	n/a	~ 0 ns	n/a	n/a	~ 0 mHz
Root sum square			24–51 ns[a,c]			5.0 mHz[a,c]
			9.2 ns			1.4 mHz

[a] Without phase calibration.

[b] Not applicable.

[c] Without S/X calibration of the ionosphere.

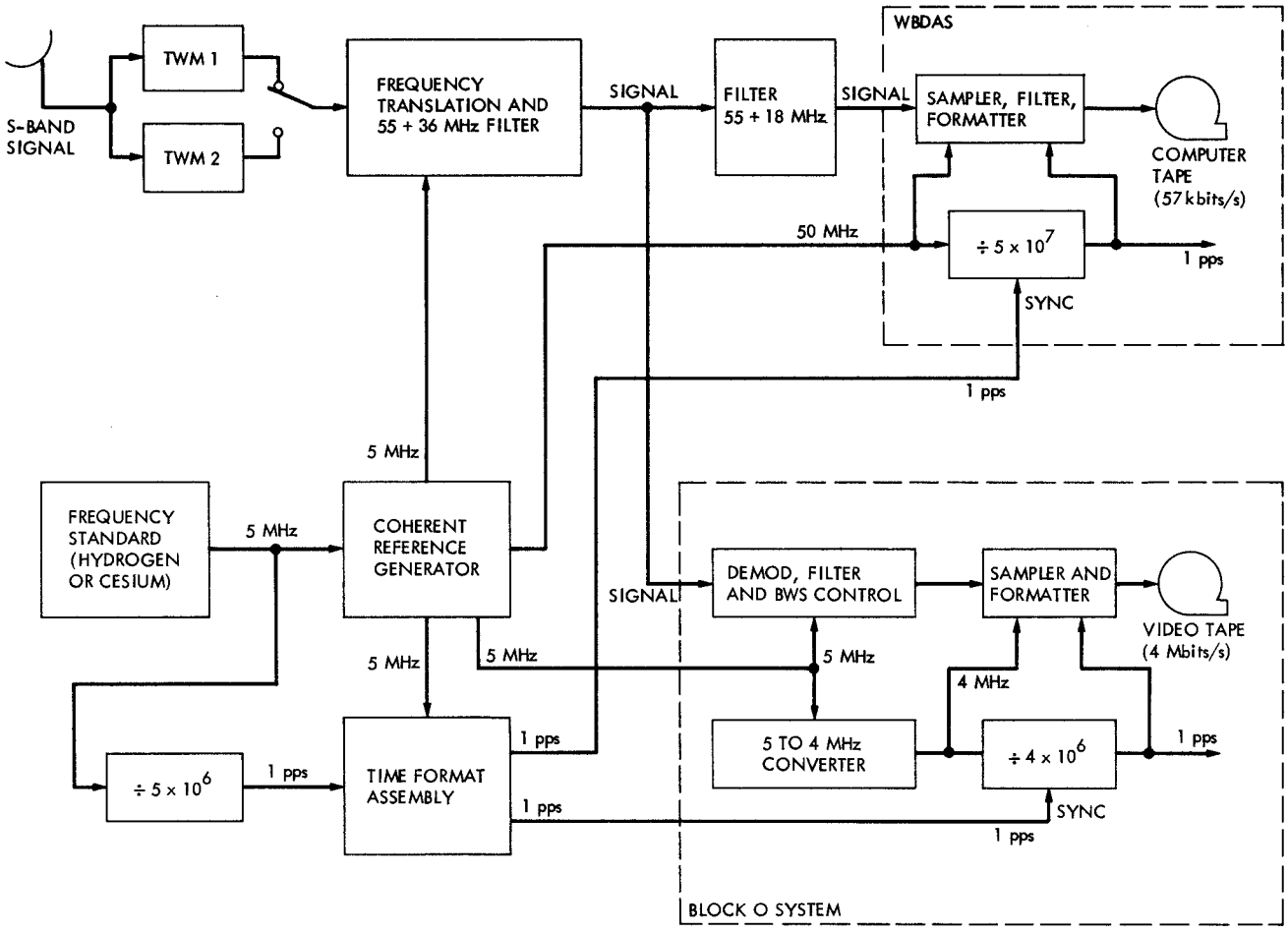

Fig. 1. Configuration of VLBI systems in Deep Space Station

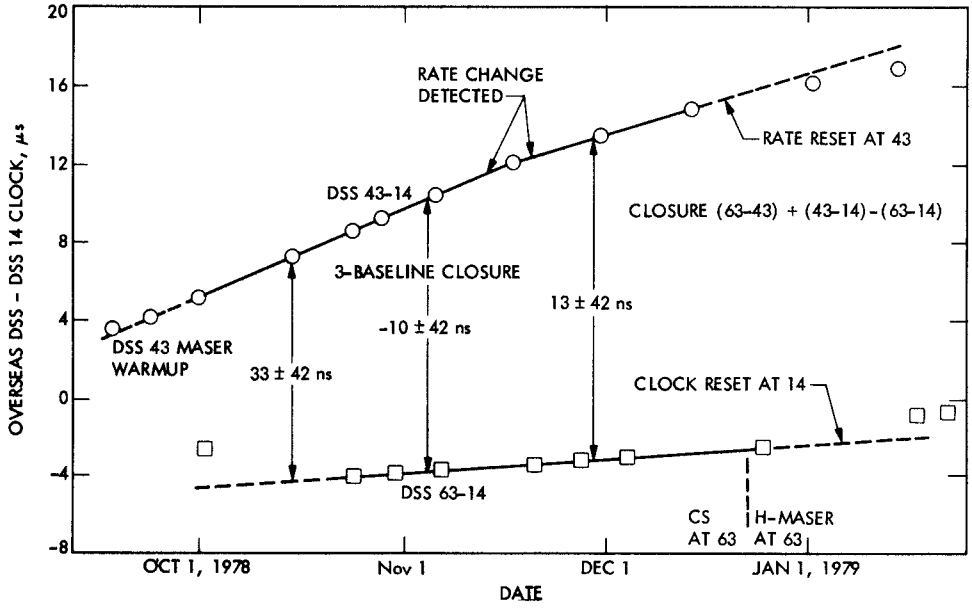

Fig. 2. Clock offsets and closure

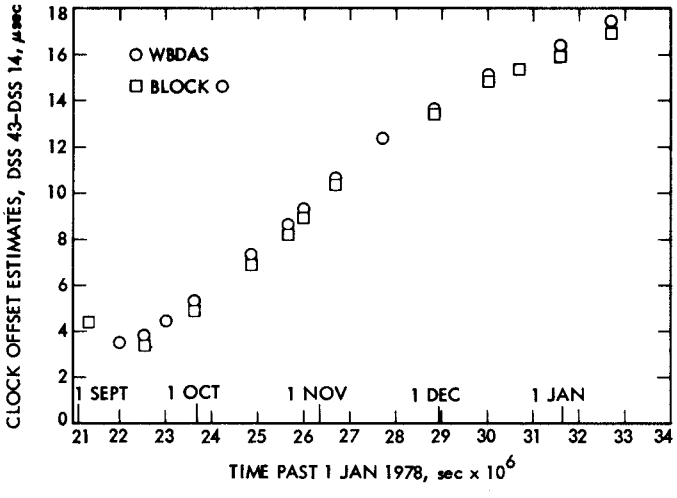

Fig. 3. Clock offset estimates, DSS 43 minus DSS 14

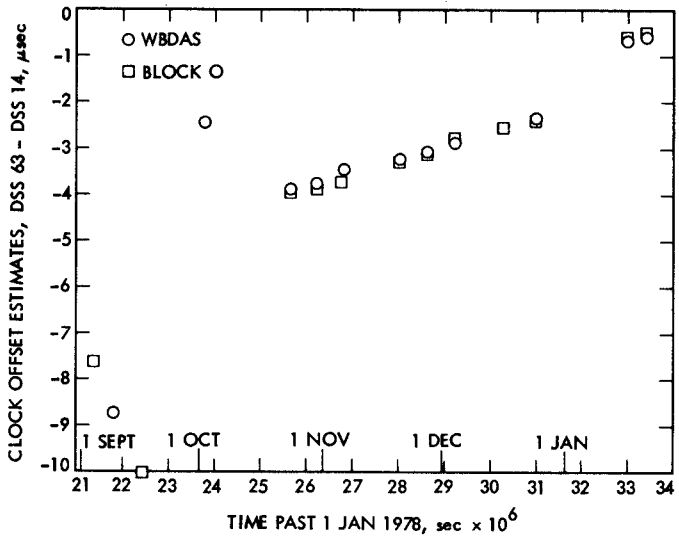

Fig. 4. Clock offset estimates, DSS 63 minus DSS 14

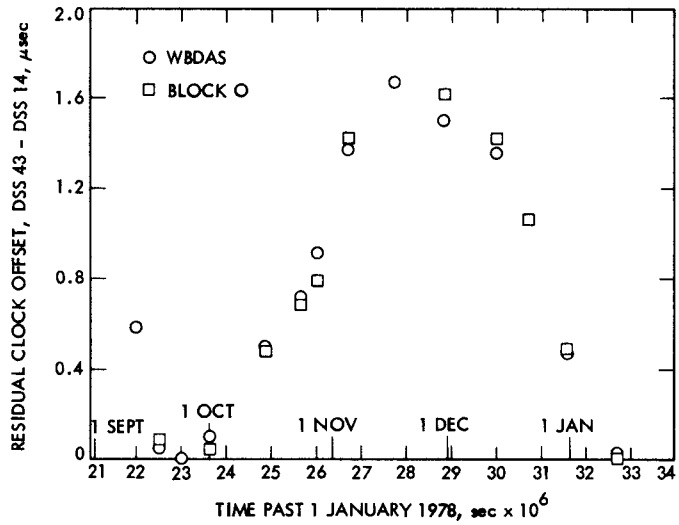

Fig. 5. Residual clock offset estimates, DSS 43 minus DSS 14

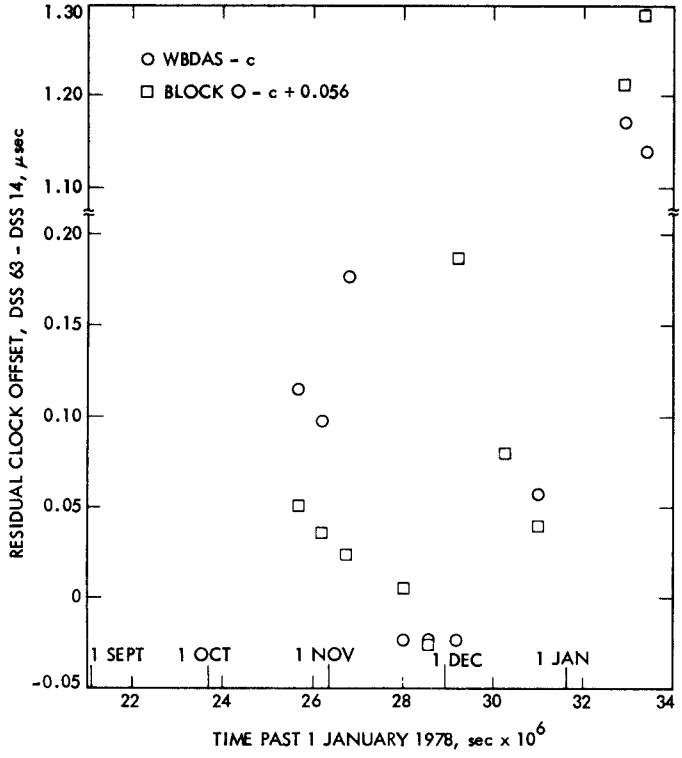

Fig. 6. Residual clock offset estimates, DSS 63 minus DSS 14